https://dx.doi.org/10.6092/10446_27138

WATER DROP IMPACT INTO A DEEP POOL: INFLUENCE OF THE LIQUID POOL TEMPERATURE

Stephanie Fest-Santini[1,C], Manfredo Guilizzoni[2], Maurizio Santini[1], Gianpietro Elvio Cossali[1]

[1] Department of Industrial Engineering, University of Bergamo, viale Marconi 5, 24044 Dalmine (BG), Italy
[2] Department of Energy, Politecnico di Milano, via Lambruschini 4, 20156 Milan, Italy
[C]Corresponding author: stephanie.fest-santini@unibg.it

ABSTRACT
The cratering regime with its manifold characteristics like micro-entrapments, primary entrapment which could lead to the trampoline phenomena, vortex rings, micro-jetting and thick jets is chosen as a study case for the influence of liquid pool temperature on the drop impact into a deep pool. Characteristic drop impact which features micro-entrapments, primary entrapment and trampoline phenomena are selected as a test cases. Pool temperatures between 20 and 40 °C are studied, whereby the droplet temperature is kept constant. The experimental results are compared with simulations obtained using the *interFoam* solver of the OpenFOAM® open source CFD package.

INTRODUCTION

The impact of a drop onto a deep liquid layer produces an amazing amount of different phenomena, like coalescence, splashing, bubble entrapment, crater formation, vortex rings, etc. Comprehensive reviews can be found in [1-3]. Several classifications of the drop impact regimes are proposed by many authors of the occurring phenomena based on dimensionless numbers, like Weber and Froude, using thermophysical parameters of impacting drops. The influence of viscosity and/or surface tension on impact outcomes is usually studied altering both drop and pool liquid [4], so that pool and impacting drop offer equal properties. It has been observed [5] that variations of bath temperature can influence the vortex penetration depth, especially, for impacting water drop into water pool. This is likely due to the change of viscosity due to its strong temperature-dependency. However, thermophysical properties of the liquid pool do not define dimensionless numbers and consequently do not influence the classification or description of impact outcomes, but may affect the impact phenomena.

This paper is aimed to study experimentally and numerically the influence of the liquid pool temperature on the crater evolution and its surrounding phenomena like micro-entrapment and trampoline phenomena. The work consists of two conceptual parts. The first one is aimed to verify if CFD solvers may be able to reproduce the complex phenomena which are observed during deep pool impacts, and particularly the effect of temperature on the crater shape and evolution. The *interFoam* solver of the OpenFOAM® CFD package [6] is selected for the numerical simulations since promising results are obtained in the field of drop impact onto liquid films and pools [7-12]. The second aspect of the investigation is related to the influence of liquid pool temperature on impact phenomena observed in classical experiments. The complementary numerical, easily accessible information, like velocity or pressure field, may help to understand physically the observed outcome.

EXPERIMENTAL METHOD

Drop impact experiments are carried out at the Department of Industrial Engineering, University of Bergamo, whereby the high-speed visualisation techniques with continuous back-light illumination is used to observe droplet impacts into a pool of the same liquid. Millimetric water droplets are generated by an on-demand droplet generator. The drops fall by gravity onto a deep (i.e. depth much larger of drop diameter) water pool crossing an optical trigger device that produce a TTL pulse. This pulse triggers the acquisition of the high speed camera.

Special accuracy is required in the alignment of the water level in the pool and camera position in relation to the water level. Otherwise, refractive and alignment distortions or black stripes within the images due to liquid interfacial phenomena with the pool walls (meniscus) appear. It is worth noting that the dimension of black stripes depends also from the thickness of the pool walls and can only be avoided by a correct and constant water level in the pool. Thereby, the pool is connected to a level water container mounted on a micrometric stage. The micrometric stage allows a precise regulation of the water level, whereby the large surface area of the level pool guaranties its constancy during experiments. Additionally, the camera is mounted on a tilting, rotating and movable platform, so that its lens axis can be independently adjusted.

To increase the degree of observation within the droplet [10], the distance between impact point and camera-facing pool wall is reduced, so that wall effects should be considered for later times after impact.

The recorded images are post-processed to obtain the crater interface as function of time. Hereby, the algorithm comprises background subtraction, contrast enhancement, image cleaning and edge detection using the Laplacian of Gaussian (LoG) method and feature detection. The contrast enhancement including lower and high upper limits of the intensities setting and the intensification factor are adapted to the detectable information. Each experimental investigation is analysed by extracting the following information: (a) impact velocity, diameter and sphericity using the frames before drop impact, (b) crater interface contour as function of time and (c) the quantity and contour of entrapments as function of time.

The temperature of the bath is adapted in the range between about 20 and 40 °C with the aim to vary its thermophysical properties (table 1). Each impact event is repeated three times for statistical reasons at equal pool liquid temperature.

Table 1: Thermophysical properties of water in the applied temperature range

T [°C]	ρ [kg/m^3]	η [kg/(m s)]	σ [N/m]
20 ± 0.5	999.21	$1002.0 \cdot 10^{-6}$	$72.44 \cdot 10^{-3}$
40 ± 0.5	992.22	$653.2 \cdot 10^{-6}$	$69.53 \cdot 10^{-3}$

NUMERICAL METHOD

Hardware and software

The simulations are performed at the Department of Engineering, Politecnico Milano, on a notebook PC with a Intel Core i7-740QM CPU (4 cores @ 1.73 GHz, 8 threads) with 6 GB RAM and on a desktop PC with a Intel Core i7-990X CPU (6 cores @ 3.46 GHz, 12 threads) with 24 GB RAM, both with Ubuntu Linux as the operating system.

Concerning the used software, *interFoam* is a two-phase isothermal finite volume solver which uses a Volume of Fluid (VOF) [13] approach modified with the introduction of an additional term in the volume fraction equation, to obtain interface compression by means of a tuneable parameter. The continuum surface force (CSF) model [14] is used to include surface tension at the interface. A detailed descriptions of *interFoam* and of the underlying models can be found in [7, 8, 15 - 19]. During preliminary tests, OpenFOAM® versions 1.7.1 and 2.1.x gave practically identical results concerning the crater shape, while significant differences were found (despite the use of the same mesh, schemes and settings) for the entrapped bubble, whose existence and dynamics are much better captured by version 1.7.1. Further investigation is at present being carried out to understand this strange behaviour. For this work, version 2.1.x is used.

Model and settings

No modifications were done to the solver for the present simulations and the discretization schemes and settings from the official *damBreak* tutorial case are in general used. The domain is modeled and meshed with the *blockMesh* OpenFOAM® utility. Domain dimensions are 0.02 x 0.02 x 0.015 m in 3D cases and 0.02 x 0.02 m x 5° in the 2D axisymmetric cases. In all cases the boundary conditions are defined as follows:

- wall boundary for the front, back, bottom and external sides of the pool;
- open boundary for the top of the domain ("atmosphere");
- axial symmetry for the axis in the axisymmetric case;
- symmetry plane for the internal "side" of the mid-pool in the 3D case.

Water drops with different diameters, velocities and temperatures were used, in all cases with dry air at the drop temperature as a surrounding medium. Both fluids are assumed Newtonian and incompressible and the flow laminar. Water regions are initialized using the *setFields* and *funkySetFields* OpenFOAM® utilities.

The solver is let free to adapt the time step to keep the Courant number under 0.5. Such requirement is the limit for 2D simulations using the scheme implemented in OpenFOAM® and should be reduced to under 0.3 for 3D cases [17, 18]. The problem is partially addressed by the introduction of some volume fraction sub-cycles, because obviously a very low value of the Courant number would imply very small time steps and consequently extremely long simulations.

Preliminary tests

During the experiments, the distance between the impact point and the camera-facing pool wall has to be quite small to allow a very detailed observation of the phenomena happening within the droplet. The negative counterpart is that wall effects on the crater evolution can only be neglected for the initial stage of drop impact. Moving to the numerical world, the consequence is that a 2D axisymmetrical simulation (with all its benefits in terms of required resources and simulation time) may not give adequate results. The first performed test is therefore a comparison between a 3D simulation and a corresponding 2D axisymmetrical simulation, to evaluate up to which time they show good agreement. Figure 1 shows the results. As for all the cases described in the paper, the drop surface is extracted as the isosurface for volume fraction equal to 0.5. No significant difference appears if other values in the range 0.1-0.9 are used. Cross-sections of such isosurface are then extracted when needed, as in this case. The hypothesis of axisymmetry appears to be acceptable for the initial part of the impact, which is the most interesting for this work.

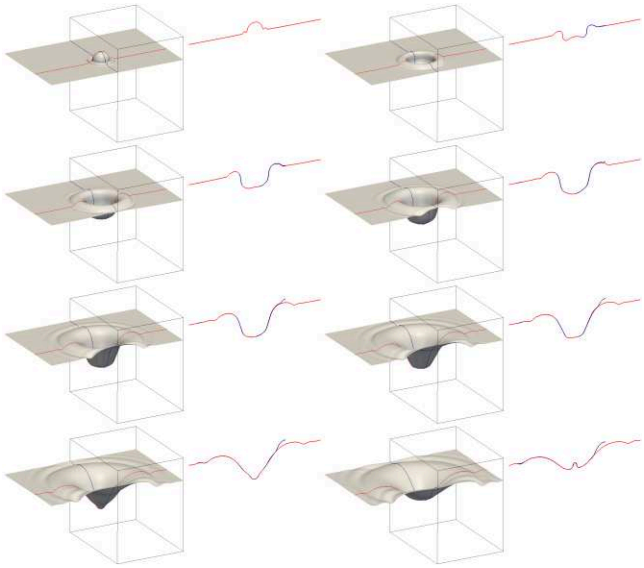

Figure 1: results of the 3D numerical simulation, where two orthogonal cross-sections are evidenced to verify the axisymmetry hypothesis. Time = 1.5 :3 : 22.5 ms (row-wise) from the beginning of the simulation. Mesh: 160 x 160 x 160 cells.

Then, a suitable 2D axisymmetric mesh is searched for. The selected mesh, which will be used as the base mesh for the simulation presented hereafter, is purely structured and composed by hexahedral and wedge elements, with grading in both direction. It is sketched in figure 2 (to increase

visibility, in the figure the mesh resolution is reduced 5 times in each direction with respect to the real one).

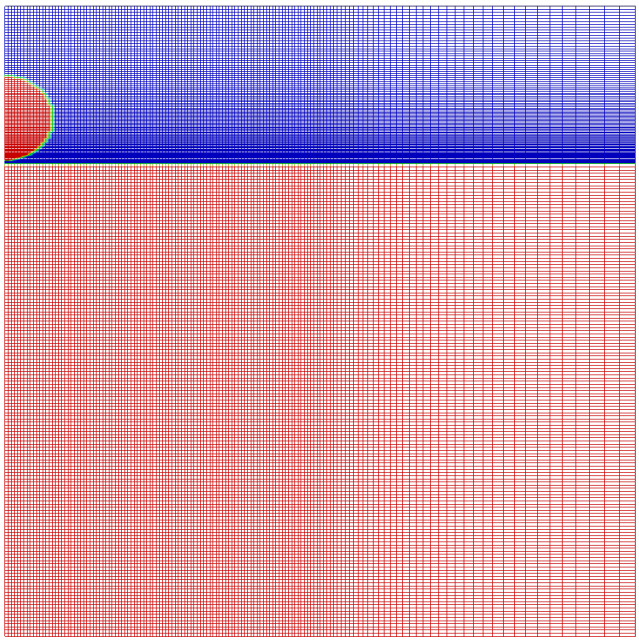

Figure 2: Reference mesh structure for the axisymmetric cases, and initial setting of the volume fraction (red = water, blue = air). Mesh resolution has been decreased 5 times with respect to the real one to improve visibility. The real mesh is 700 x 950 x 1 (665000) cells.

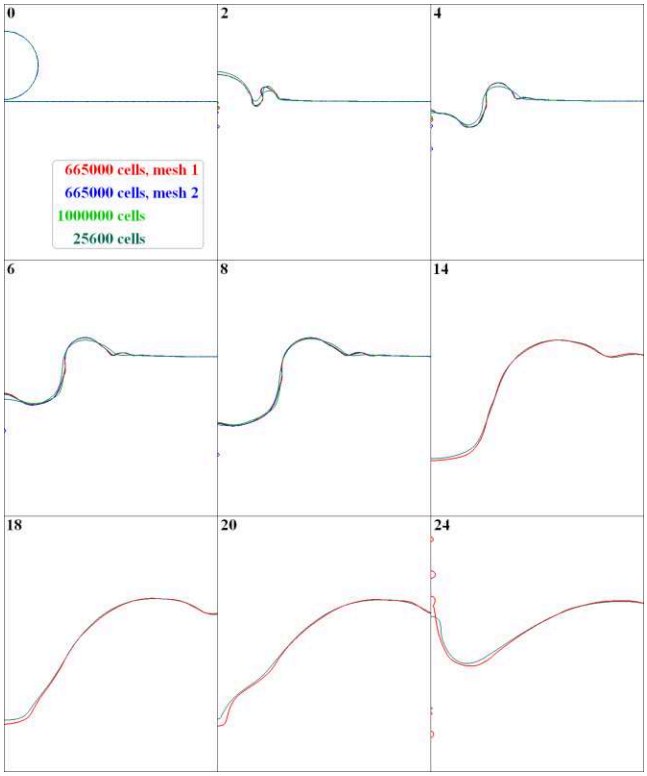

Figure 3: Mesh independence of the numerical crater evolution. Time [ms] from the beginning of the simulation is indicated in the upper left corner of each frame.

Mesh independence of the results is then analyzed on a test case characterized by drop diameter 3.5 mm, drop speed 1.14 m/s, drop temperature 26 °C. Good mesh independence is found, even if the finest structures (bubbles, micro-jetting) are lost with the roughest mesh. Figure 3 shows the results. Finally, some tests are performed to evaluate if the "default" value of the Courant number may be adequate. The discretization schemes proposed in the official *damBreak* tutorial seems to be already a good choice, apart from the temporal discretization which is only first order. Therefore, a test is also performed by replacing it with a Crank-Nicholson "0.5" scheme. Slight improvement is found for some details, but in general no significant difference may be noticed (figure 4), while simulation time with the modified settings is more than 4 times longer (and over one order of magnitude longer for some time steps).

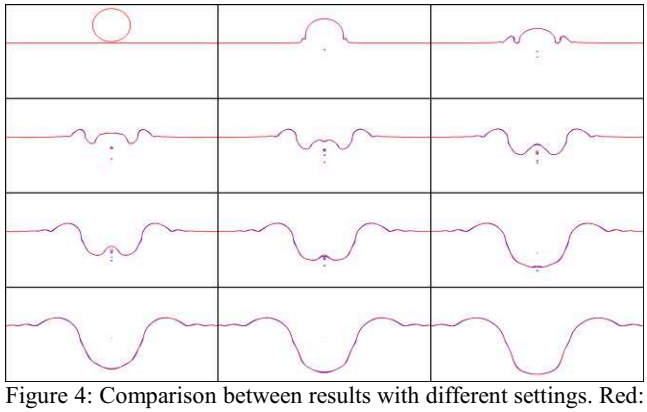

Figure 4: Comparison between results with different settings. Red: Euler time discretization, Co = 0.5, 3 volume fraction sub-cycles; blue: Crank Nicholson "0.5" time discretization, Co = 0.05, 5 volume fraction sub-cycles. Time: 0: 0.8 : 8.8 ms from the beginning of the simulation.

RESULTS

As test cases to verify the performance of the CFD solvers, selected mesh and settings, the impact of a drop having diameter 2.95 mm and impact velocity 1.05 m/s is chosen. The drop temperature is fixed to 24 C± 1°K and the pool temperature amounts 24°C and 40°C, respectively. Figure 5 and figure 6 shows the results superposed to experimental acquisitions for T_{pool} = 24 °C and T_{pool} = 40 °C, respectively. Both test cases do not feature the trampoline phenomena, since *interFoam* is a two-phase solver and cannot distinguish between drop water and pool water after contact. As reported in table 1, the dynamic viscosity of pool water differs of about 30% for the two test cases. This leads to slightly larger depth and faster recoil at higher pool temperatures in the experiments. But, this influence is within the experimental repetition fluctuation. The entrapment of initial air bubbles - produced by rupture of the thin air sheet which remains entrapped between impacting drop and pool - seems to be unaffected by the variation of bath temperature. Their carrying deep within the pool is influenced by the vortex formation which is visible coloring the impacting drop [20]. This also explains their often chaotic motion (compare figure 8). The entrapment of micro bubbles too is further detailed in figure 8, where the image intensity is adapted on the visibility of entrapments.

From the numerical point of view, it may be stated that the solver is able to reproduce quite well the experimental crater shape and evolution, even if some delay in the latter is present, with consequent imperfect overlapping of the results. Part of such disagreement may be also due to the

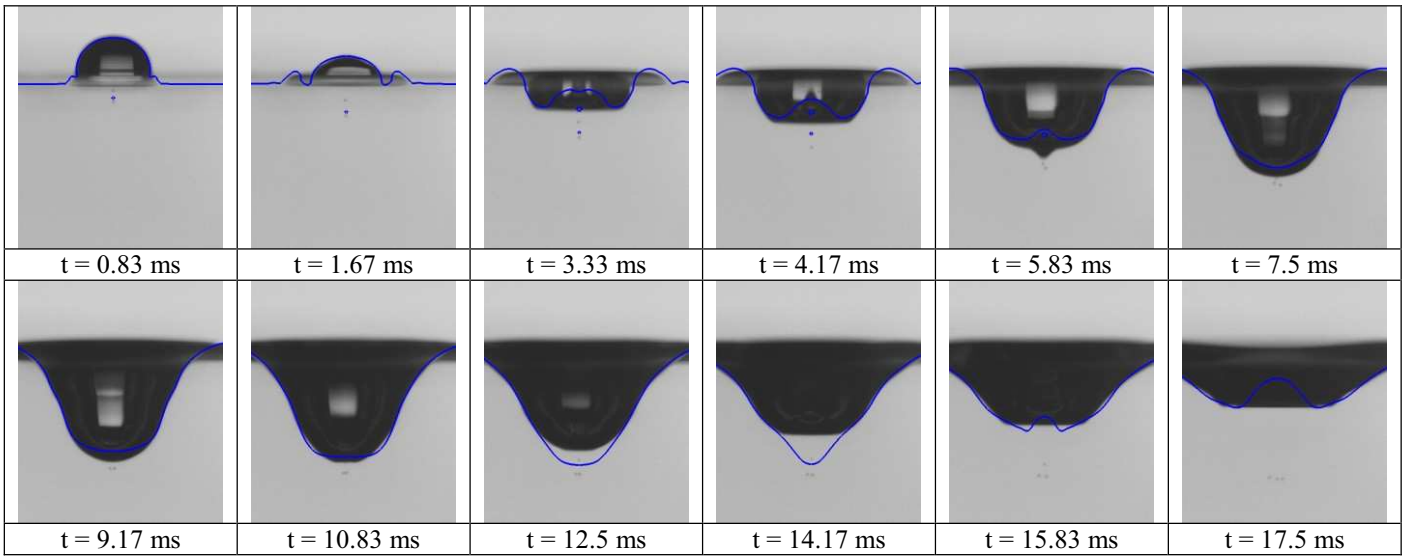

Figure 5: Superposition of the numerical crater profile to the experimental acquisition for D = 2.95 mm, V = 1.05 m/s and T_{pool} = 24°C

fact that the simulation outputs are saved every 10^{-4} s, which does not allow perfect temporal superposition with experimental frames.

As regards the dynamics of the entrapped bubbles (apart from the aforementioned comment about different results between 1.7.1 and 2.1.x OpenFOAM® versions), the immediate coalescence when they are reached by the crater is inherent in the VOF method [21], so bubble displacement by direct contact with the crater interface cannot be observed in simulation. Their lower sinking speed compared to the experimental one may on the contrary be due to the fact that in 2D axisymmetric simulations they are perfectly on the axis, so they are influenced by the center of the crater which is the last part of the latter to move downward. In experiments they may be slightly shifted from the axis, thus experiencing an earlier and stronger downward thrust.

It should be mentioned that altering the liquid properties during the numerical studies, both drop water and pool water properties are changed (again due to the fact that *interFoam* is a two-phase isothermal solver) in difference to experimental approach. Concerning specifically the temperature influence, it can be seen from figure 5 and figure 6 how the first part of the evolution is almost perfectly superposed. Then at the higher temperature the crater reaches a larger depth and recoils faster and with a smaller central cone. A similar, but less pronounced, tendency is also observed experimentally.

The difference of surface temperature of impacting drop and liquid pool could lead to the trampoline phenomena. A series of capillary waves propagates up the impacting drop and converges at its top, pinching off a smaller secondary drop. As shown in detail in figure 7, the secondary drop falls onto the bottom of the crater and is then ejected by the receding crater. This ejection affects the crater shape. Main differences are observed at about 6 ms and 7°ms (expanding crater) and again at about 12 ms and 13 ms (receding crater) after drop impact. Increased surface temperature facilitates the trampoline phenomena, but it seems to be not the only requirement (compare figure 6). Bisighini [23] has reported that a prolate shape of the impacting drop may cause the trampoline phenomena. This observation could not be confirmed as main condition. The ejection of a secondary drop has been observed for prolate as well as for oblate drop shapes and the liquid pool temperature was always higher than 30°C.

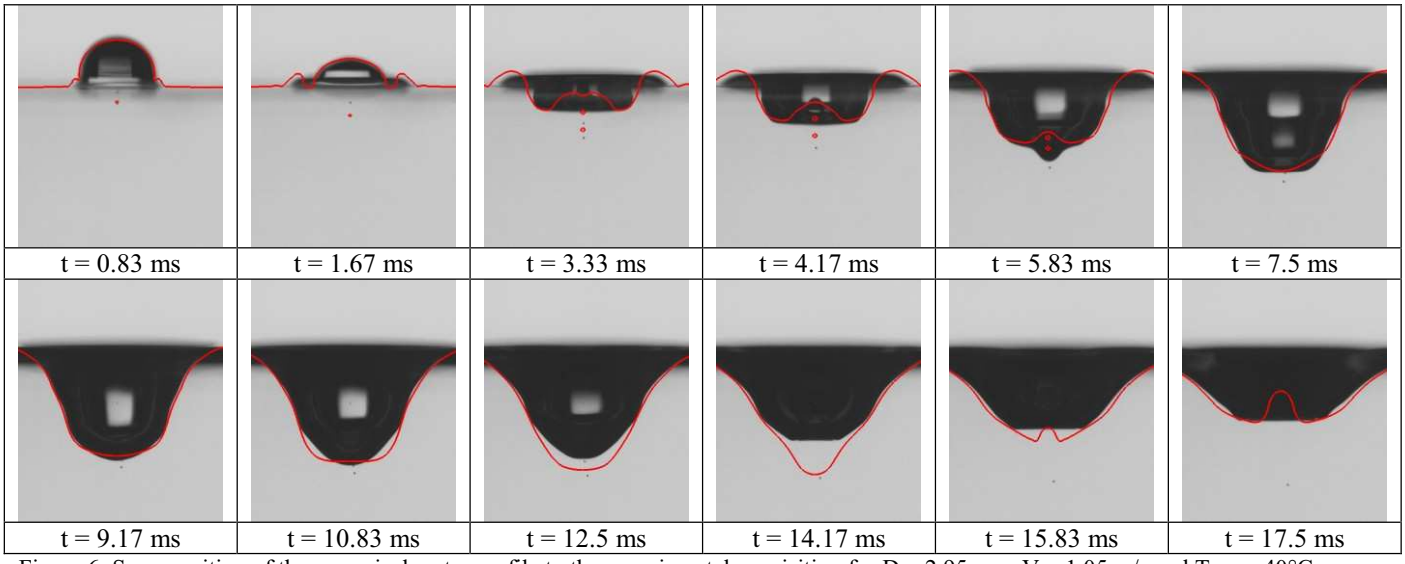

Figure 6: Superposition of the numerical crater profile to the experimental acquisition for D = 2.95 mm, V = 1.05 m/s and T_{pool} = 40°C

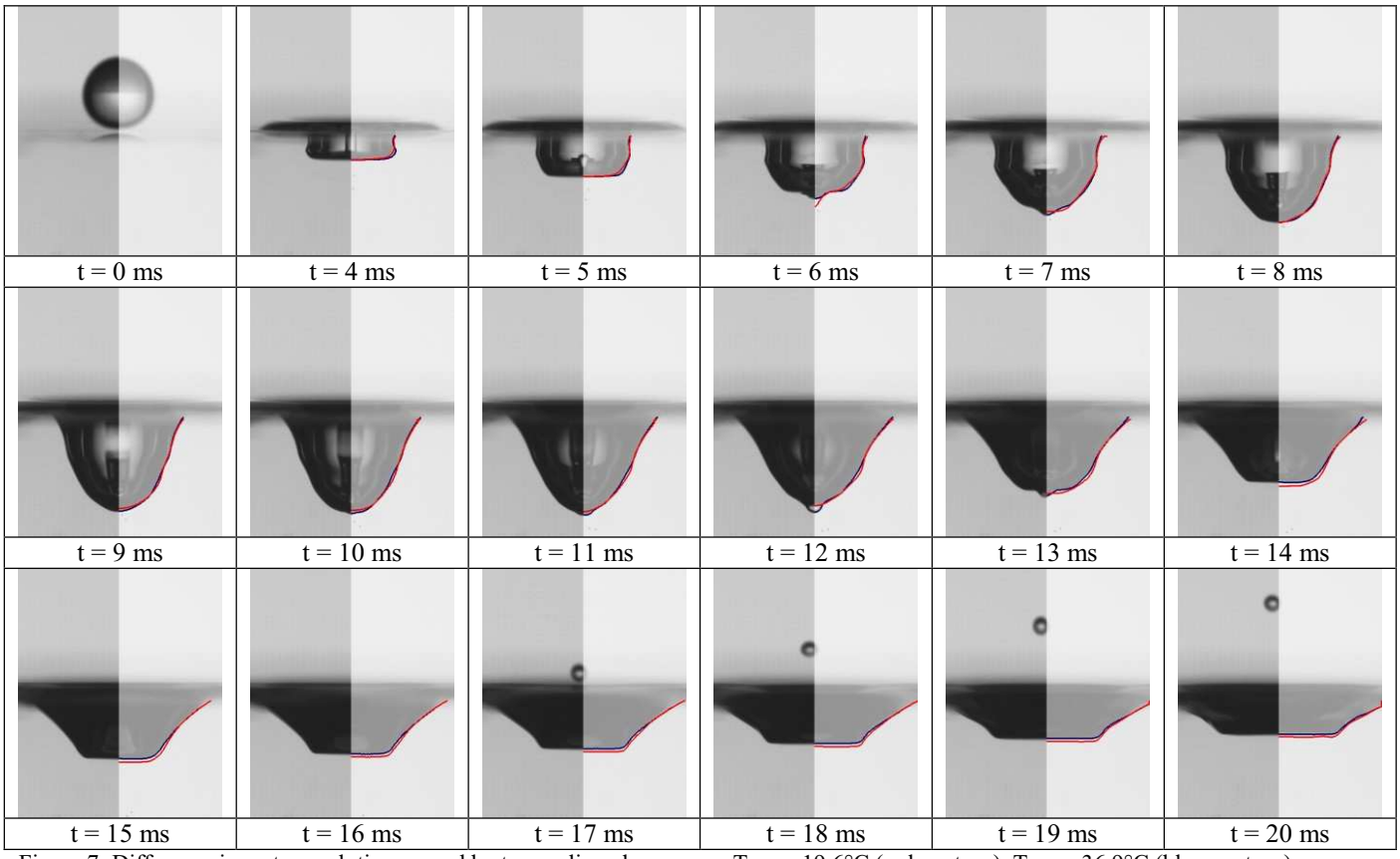

Figure 7: Difference in crater evolution caused by trampoline phenomena: T_{pool} = 19.6°C (red contour), T_{pool} = 36.9°C (blue contour)

Figure 8 shows the evolution of micro-bubbles entrapment of drop impact shown in figure 5. The intensity profile is adapted with the focus on the visualization of entrapped micro-bubbles (figure 8, left side) and afterwards the images are binarized (figure 8, right side). As shown in figure 5 and figure 6, a secondary drop is formed within the crater in analogy to the trampoline phenomena. This drop is not ejected by the receding crater; it is disgorged by the still expanding crater at times of about 6 ms after impact. The crater itself is characterized to that time by a tip. The secondary drop is carried deep inside the pool liquid as shown in figure 9 for times later than 12.5 ms after impact. At earlier time, the disgorged drop is covered by the expanding crater and is not visible in the projected view of the high speed image. The disgorging of the secondary droplet is observed for all tested liquid pool temperatures. It seems to be that the secondary droplet within the crater is always formed and is either disgorged or ejected and the crater shape is governed by one or the other phenomena (see figure 7). The probability of secondary droplet ejection increases with increasing liquid pool temperature which corresponds to an increased difference in dynamic viscosity between impacting drop and pool water.

The test simulations do not predict a secondary drop formation, so that neither the ejection upwards (trampoline) nor the disgorging downward in the pool liquid could be numerically described.

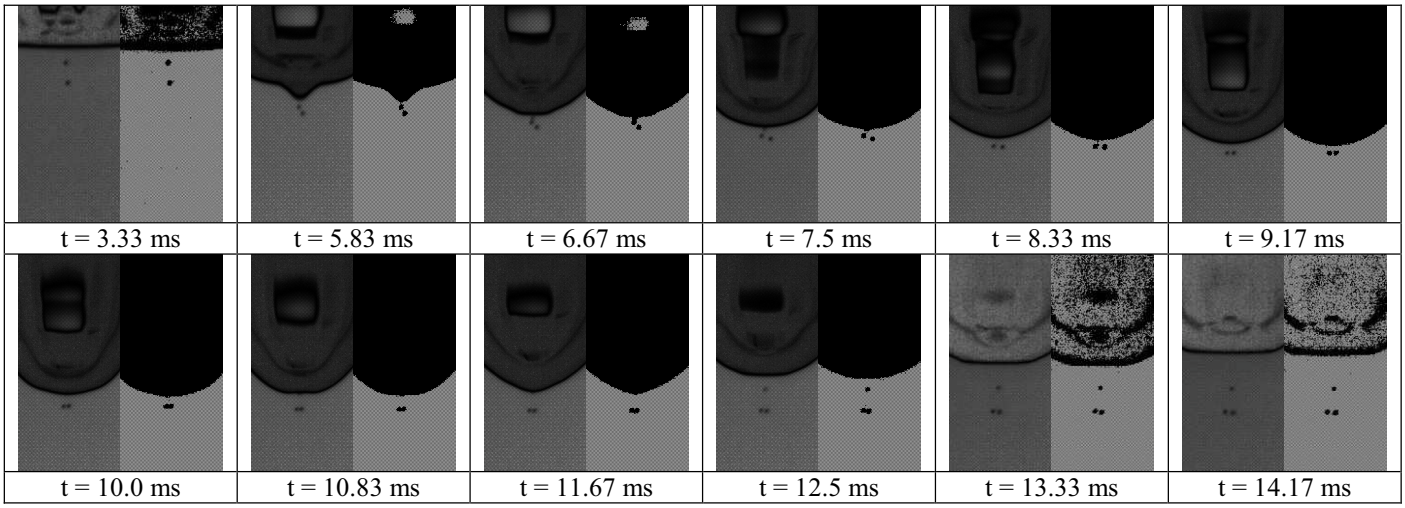

Figure 8: Additional bubble entrapment caused by entrapped drop in crater for D = 2.95 mm, V = 1.05 m/s and T_{pool} = 24°C (impact conditions of figure 5): intensity adapted (left side of each image) and binary images (right side of each image)

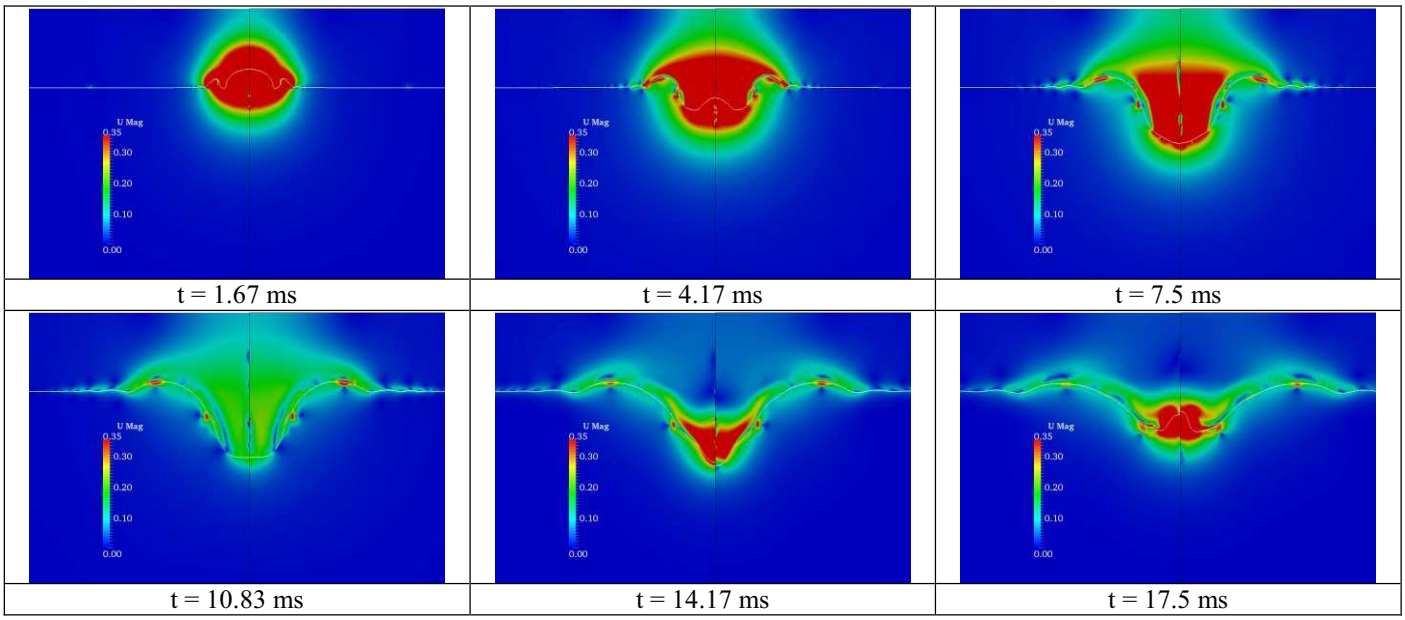

Figure 9: Velocity magnitude calculated by numerical simulation for two test cases for D = 2.95 mm, V = 1.05 m/s and T_{pool} = 24°C (left side of each image) and T_{pool} = 40°C (right side of each image)

Figure 9 shows the comparison between the two numerical test cases T_{pool} = 24 °C and T_{pool} = 40 °C in terms of velocity magnitude. The color scale of the velocity magnitudes is limited between 0 m/s and 0.35 m/s for visibility reasons and velocity profiles below the crater are very similar for both test cases due to the similar crater shape.

A peculiar phenomenon is that of the fast upward jets which can be observed when the crater reaches and incorporates the entrapped bubbles. Such behavior is quite strange and it may be an effect of numerical problems, but it may also have a physical meaning, being related to the capillary pressure within the bubbles. Their radius is between $5e^{-5}$ and $1e^{-4}$ m, resulting in a capillary pressure predicted by the Laplace-Young equation (for spherical bubbles) between 2900 Pa and 1400 Pa (in perfect agreement with the simulated values which are between 3000 Pa and 1400 Pa). When the bubbles coalesce into the crater, the above air is projected upwards.

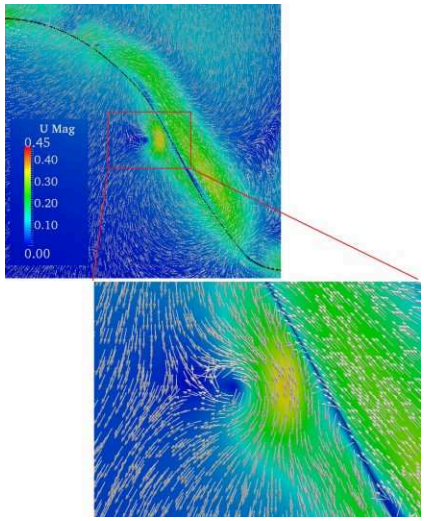

Figure 10: Numerical predicted vortex structure that develops along the crater side (T_{pool} = 24 °C, t = 12.5 ms)

Another interesting phenomenon which could be numerically predicted is the vortex that develops along the crater side (figure 10). This vortex structure at the crater side was visualized dying the impacting drop [20].

CONCLUSION

A comparative study of experimentally and numerically obtained drop impacts into deep pools in the cratering regime aimed to identify the dependence of liquid pool temperature on drop impact phenomena was performed.

The crater shape is influenced by the upward (ejected) or downward (disgorging) motion of secondary drop formed within the crater within the expanding phase. Ejection is facilitates at higher pool liquid temperature.

The *interFoam* solver seems to be a suitable tool for the simulation of drop impacts into pools. Phenomena like trampoline (ejection) or disgorging of the secondary drop and the corresponding influence on the crater shape could not be predicted as they require the utilization of a multi-phase solver.

REFERENCES

[1] Rein, M., *Phenomena of liquid drop impact on solid and liquid surfaces*, Fluid Dyn Res, 1993, 12, pp. 61-93.

[2] Rodriguez, F., Mesler, R., *The Penetration of Drop-Formed Vortex Rings into Pools of Liquid*, J Colloid and Interface Sci, 1988, 121, pp. 121-129.

[3] Yarin, A.L., *Drop impact dynamics: splashing, spreading, receding, bouncing,* Annu Rev Fluid Mech, 2006, 38, pp. 159–192.

[4] Deng, Q., Anilkumar, A.V., Wang, T,G., *The role of viscosity and surface tension in bubble entrapment during drop impact onto a deep liquid pool*, J Fluid Mech, 2007, 578, pp. 119–138.

[5] Peck, B., Sigurdson, L, *The three-dimensional structure of an impacting water drop*, Phys Fluids 1994, 6, pp. 564-576.

[6] *OpenFOAM®*, The open source CFD toolbox, website: http://www.openfoam.com/, accessed March 2012.

[7] Costa A.B., Graham Cooks R., *Simulated splashes: Elucidating the mechanism of desorption electrospray ionization mass spectrometry*, Chemical Physics Letters, 2008, 464, 1-8.

[8] Berberovic E., van Hinsberg N.P., Jakirlic S., Roisman I.V., Tropea C., *Drop impact onto a liquid layer of finite thickness: Dynamics of the cavity evolution*, Physical Review E 79, 036306, 2009.

[9] Roisman I.V., Berberovic E., Jakirlic S., Tropea C., *Dynamics of two-phase flows induced by drop collisions*, Proceedings of the 7th International Conference on Multiphase Flow (ICMF), Tampa (FL,USA), 2010.

[10] Fest-Santini S., Guilizzoni M., Santini M., Cossali G.E., *Drop impacts in pools: a comparison between high speed imaging and numerical simulations*, Proceedings of the Droplet Impact Phenomena & Spray Investigations (DIPSI) Workshop 2011, Dalmine (Italy).

[11] Santini M., Fest-Santini S., Guilizzoni M., Cossali G.E., *Drop impact onto a deep pool: study of the crater evolution*, Proceedings of the 24th European Conference on Liquid Atomization and Spray Systems (ILASS - Europe 2011), Estoril (Portugal), 2011.

[12] Berberovic, E., *Investigation of Free-surface Flow Associated with Drop Impact: Numerical Simulations and Theoretical Modeling*, Ph.D. Thesis, TU Darmstadt, 2010

method for the dynamics of free boundaries, Journal of Computational Physics, 1981, 39, 201-225.

[14] Brackbill J.U., Khote D.B, Zemach C., *A Continuum Method for Modeling Surface Tension*, Journal of Computational Physics, 1992, 100, 335-354.

[15] *The OpenFOAM® User Guide*, available online at website: http://www.openfoam.org/docs/, accessed July 2012.

[16] Weller H.G., Tabor G., Jasak H., Fureby C., *A tensorial approach to computational continuum mechanics using object-oriented techniques*, Computer in Physics, 1998, 12(6), 620-631.

[17] Jasak H., Weller H.G., *Interface-tracking capabilities of the InterGamma differencing scheme*, Technical Report, Imperial College of Science, Technology and Medicine, University of London, 1995.

[18] Gopala V.R., van Wachem B.G.M., *Volume of fluid methods for immiscible-fluid and free-surface flows*, Chemical Engineering Journal, 2008, 141, 204-221.

[19] Ferziger J.H., Peric M., Computational Methods for Fluid Dynamics, 3rd Ed., Springer, 2002.

[20] Santini, M., Fest-Santini, S., Cossali, G.E., *LDV characterization of the liquid velocity field underneath an impacting drop*, 16th Int. Symp. on Appl. Laser Techniques to Fluid Mechanics, Lisbon (Portugal), July, 2012.

[21] Nikolopoulos N., Nikas K.-S., Bergeles G., *A numerical investigation of central binary collision of droplets*, Computers & Fluids, 2009, 38, 1191-1202.

[22] Bisighini, A., *Single and double drop impact onto a deep and thick liquid layer*, Ph.D. Thesis, University of Bergamo, 2009.